Journal of
Ceramic Science
and Technology

J. Ceram. Sci. Tech., **01** [01] 41-50 (2010)
DOI: 10.4416/JCST2010-00001
available online at: http://www.ceramic-science.com

Effect of CdO Addition on the Microstructure and Microwave Dielectric Properties of $Ba_xSr_{1-x}TiO_3$ Ceramics

Doaa A. Abdel Aziz[1], Wagdy N. Nour[1], Aisha E. Reda[1], Eglal R. Souya[2]

[1]Ceramic Department, National Research Centre, 12622, Dokki, Cairo, Egypt
[2]Chemistry Department, Faculty of Science, Ain Shams University, Cairo, Egypt

received February 13, 2010; received in revised form March 25, 2010; accepted April 11, 2010

Abstract

Ceramic-based barium strontium titanate (BST) solid solutions with the formula $Ba_xSr_{1-x}TiO_3$ are very important candidates for millimetre-wave applications (e.g. filters and antennas). Several samples with and without CdO were prepared by means of the conventional solid-state route. Five compositions with ($0.00 \leq x \leq 0.30$) sintered at temperatures in the range 1300 - 1500 °C were investigated. Structural X-ray diffraction analysis confirmed their perovskite structure. The morphology of the sintered ceramic bodies was analysed by means of scanning electron microscopy (SEM) and energy-dispersive X-ray (EDAX) microanalysis. The cavity resonance method was used to measure the dielectric properties at microwave (MW) frequency range 40 MHz – 8 GHz. The results revealed that the microwave dielectric characteristics were strongly affected by different Ba/Sr ratios, the cadmium concentration and the microstructure developed. The addition of CdO (0.10, 0.15 and 0.20 mol %) to $Ba_xSr_{1-x}TiO_3$ ceramic bodies decreased the sintering temperature, with optimum density being obtained at 1400 °C. The best combination of microwave dielectric characteristics was obtained for BST10 ceramic with 0.20 mol % CdO sintered at 1400 °C/2 h, with dielectric constant (ε_r) = 291, low dielectric loss = 0.0005 and quality factor ($Q \times f$) = 3281 at 1.8 GHz). This can be attributed to its uniform grain morphologies and fine-grained (≤ 0.1 µm) crystalline phases that are round in shape.

Keywords: microwave, dielectric properties, microstructure, SrO, BaO, TiO_2 and CdO

I. Introduction

Novel complex perovskite materials have been recently introduced, particularly for wireless and telecommunication applications involving high-frequency operation above 1 GHz [1-6]. The new materials involve various cation substitutions at the A and B sites of ABO_3 perovskite. These substitutions have been shown to change the structural characteristics of the perovskite and consequently, the microwave dielectric properties, such as dielectric constant, dielectric loss and quality factor.

To meet popular demand, the dielectric characteristics of ceramic materials have been rapidly improved. At the same time, attempts have been made to reduce the size of all communication devices, to make them as small and as lightweight as possible. On account of this trend, high dielectric constant materials such as barium strontium titanate are becoming increasingly important in ceramic materials[7, 8]. Barium strontium titanate ($Ba_xSr_{1-x}TiO_3$, BST, $0.00 < x < 1$) is a solid solution of barium titanate and strontium titanate, which form solid solutions across the entire compositional range owing to their similar crystal structure and comparable ionic radii[9]. Measurements of reaction kinetics showed that Ba-rich BST compositions exhibited more rapid reaction rates compared with Sr-rich BST compositions, and the reaction rate increased monotonically with the Ba content[10]. The average particle size also increased with the Ba content, with the particle growth rate of $BaTiO_3$ being approximately a factor of 10 greater than that of $SrTiO_3$. Ioachim et al.[11] found that increasing the strontium content from 0.25 to 0.9 mol % in the $(Ba_{1-x}Sr_x)TiO_3$ solid solution system led to a decrease in the dielectric constant from 1600 to 200 at 1 GHz. It was also concluded that the samples with x = 0.50 and 0.75 are suitable for microwave applications. The dielectric properties of BST depend to a large extent on variations in the type and amount of impurities, particle size, degree of homogeneity, and handling procedures. Researchers have already reported attempts to decrease the sintering temperature of BST to an appropriate level. Rhim et al.[9] reported on the influence of additions of B_2O_3 on the sintering temperature of commercial BST. The addition of 0.5 wt. % B_2O_3 reduces the sintering temperature to 1150 °C, while leaving the dielectric and ferroelectric properties unchanged. Liang et al.[12] described a reduction in the dielectric constant of $Ba_{0.6}Sr_{0.4}TiO_3$ with increasing $Mn^{2+}$and Mg^{2+} doping level, where $Mn^{2+}$and Mg^{2+} act as acceptors on Ti^{4+} sites. Ioachim et al.[11] concluded that the addition of (1 wt. %) MgO and MnO led to better sintering and grain refining of $(Ba_{1-x}Sr_x)TiO_3$ (x = 0.25 - 0.90 mol %), whereas their absence induced exaggerated grain growth, leading to the formation of large-faceted grains.

The main aim of the present work is to study the effect of different concentrations of CdO on the microstructure and microwave dielectric properties of $Ba_xSr_{1-x}TiO_3$ ceramic bodies.

* Corresponding Author doaa_ziz@hotmail.com

II. Experimental

Ceramic samples were prepared according to the solid-state route. Reagent grade $BaCO_3$ (99 %), $SrCO_3$ (99 %) (S.D. Fine-Chem Limited, Mumbai, India), TiO_2 (99 %) (PRS PANREAC QUIMICA SA, Barcelona, Spain) and $Cd(NO_3)_2 .4H_2O$ (99 %) (S.D. Fine-Chem Ltd) powders as the starting materials were weighed according to the compositions ($Ba_xSr_{1-x}TiO_3$, BST). The compositions with x = 0.00, 0.10, 0.20, 0.25, and 0.30 mol were denoted as ST, BST10, BST20, BST25, and BST30, respectively. In order to improve the sintering process, CdO was added in different proportions (0.1, 0.15 and 0.2 mol %). The starting materials were thoroughly mixed in stoichiometric proportions, ball-milled in distilled water for 2 h with agate balls in a planetary mill, dried at 110 °C for 24 h and then calcined at 1150 °C for 2 h. Secondary milling of the calcined powder was performed in water for 2 h. These compositions were then mixed with 4 wt. % polyvinyl alcohol as a binder, and uniaxially pressed into pellets with a diameter of 15 mm and a thickness of 3 mm on a hydraulic press (SEIDNER; Riedlinger type, Germany) under 20 MPa pressure and heated at 550 °C for 2 h to remove the binder. The samples were sintered in the temperature range 1300-1500 °C in air for 2 h with a heating rate of 10 °C/min.

Structural analysis of samples was performed by means of X-ray diffraction (XRD) analysis in a 2θ range from 20° to 60° on a Philips Flex 2002 diffractometer with Cu Kα radiation (λ = 1.5418 Å), Ni-filter and a detector scan speed of 2°/min. Morphological investigations were conducted on thermally etched pellets by means of scanning electron microscopy (SEM) and energy-dispersive X-ray (EDAX) using a JEOL JXA-840A Electron Probe Microanalyzer, Japan, equipped with an X-ray energy-dispersive spectrometer EDAX (INCAx-sight, OXFORD). Bulk density and apparent porosity of the sintered samples were measured with the conventional liquid displacement method. Microwave dielectric resonance measurements were examined in the frequency range of 40MHz - 8GHz with a network analyzer (Model ADVANTEST R3767CH).

III. Results and Discussion

(1) Mineralogical composition

(a) *X-ray diffraction analyses*

Fig. 1 shows the x-ray diffraction patterns of $Ba_xSr_{1-x}TiO_3$ powders with (x = 0.00, 0.10, 0.20, 0.25 and 0.30 mol) calcined at 1150 °C for 2 h. The patterns reveal the formation of strontium titanate phase in the ST sample and barium strontium titanate in the other samples containing BaO as a major phase. In addition, two reflection lines are recorded at 2θ = 27.5° and 2θ = 31.8°, which can be attributed to the presence of $(SrO)_2TiO_2$ and $Sr_3Ti_2O_7$, respectively, as intermediate phases. When the stoichiometric percentage of barium in the compositions is increased, the amount of $(SrO)_2TiO_2$ decreases and no significant change in the amount of $Sr_3Ti_2O_7$ is recorded. Moreover, a small amount of unreacted TiO_2 is identified, its amount diminishing with increasing BaO content. This clearly shows that the reaction rate speeds up with the addition of BaO. Previous measurements of the reaction kinetics showed that Ba-rich BST compositions exhibited faster reaction rates than Sr-rich BST compositions, and the reaction rate increased monotonically with the Ba content[10]. The

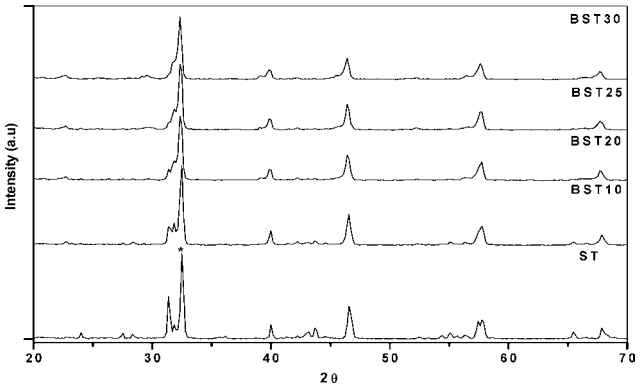

Fig. 1: XRD patterns of ST and BST calcined at 1150 °C.

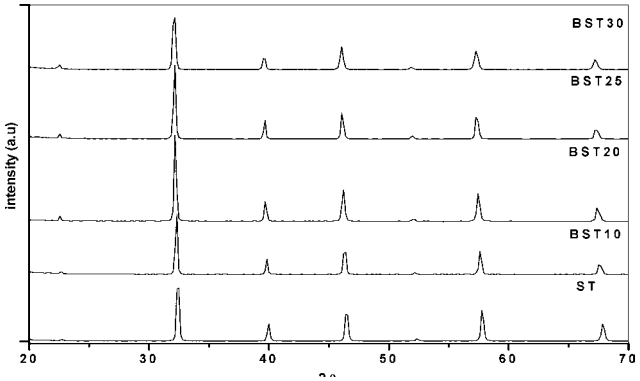

Fig. 2: XRD patterns of ST and BST sintered at 1450 °C.

XRD patterns of $Ba_xSr_{1-x}TiO_3$ ceramics with various Ba/Sr ratios sintered at 1450 °C are shown in fig. 2. All peaks show a perovskite structure. The sample (ST) with x = 0.0 has strontium titanate perovskite with a cubic structure and barium strontium titanate with tetragonal structure for the other compositions with higher x values. The peak sharpness and intensity indicate that fully crystalline phases are formed. The samples with high Ba concentration show a small shift in the XRD peaks towards lower 2θ, this is evidence of the dissolution of Ba^{2+} ions into the $Ba_xSr_{1-x}TiO_3$ structure. The shift can be explained by the fact that when barium ions are introduced at the A-site of the perovskite structure, they enter substitutionally at the Sr^{2+} site, indicating solid solubility of Ba in the ST lattice. The unit cell volume increases slightly as the Ba content increases because the ionic radius of Ba^{2+} (1.61 Å) is larger than the ionic radius of Sr^{2+} (1.44 Å), see Table 1, fig. 2 and fig. 6(a). Figs. 3, 4 and 5 show the XRD patterns of $Ba_xSr_{1-x}TiO_3$ ceramics with 0.1, 0.15 and 0.2 mol % CdO, respectively. From the figures, the single-phase formation without any impurity phase for all the Sr contents can be clearly seen. Moreover, the specimens (ST&BST10) with CdO show a shift in the position of the XRD peaks

Table 1: Change in d-spacing (2θ) of peak at 011

CdO mol%	Compositions				
	ST	BST10	BST20	BST25	BST30
0.00	32.469	32.357	32.254	32.191	32.162
0.10	32.376	32.303	32.268	32.223	32.169
0.15	32.389	32.288	32.262	32.186	32.150
0.20	32.411	32.340	32.274	32.196	32.189

to lower diffraction angle directions with the amount of CdO addition as shown in Table 1 and fig. 6 (b-d). This indicates that the Cd^{2+} cation could substitute the Ti^{4+} cation on B-site, because the ionic radius of Cd^{2+} ion (0.95 Å) is larger than that of the Ti^{4+} ion (0.61 Å).

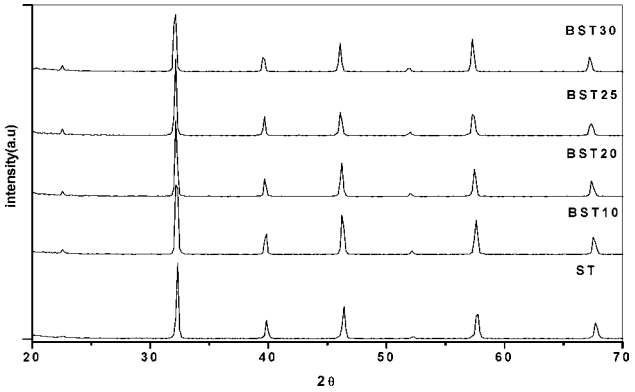

Fig. 3: XRD patterns of ST and BST with 0.1 mol% CdO as a dopant.

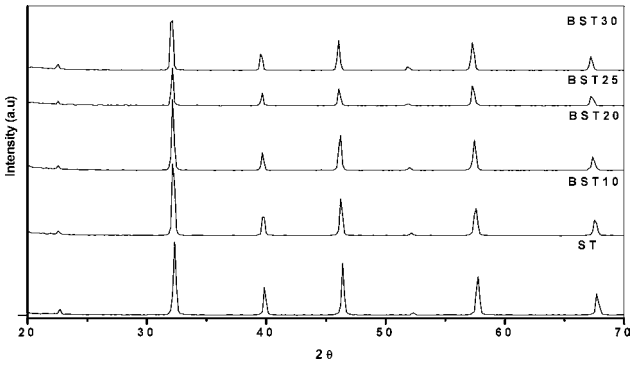

Fig. 4: XRD patterns of ST and BST with 0.15 mol% CdO as a dopant.

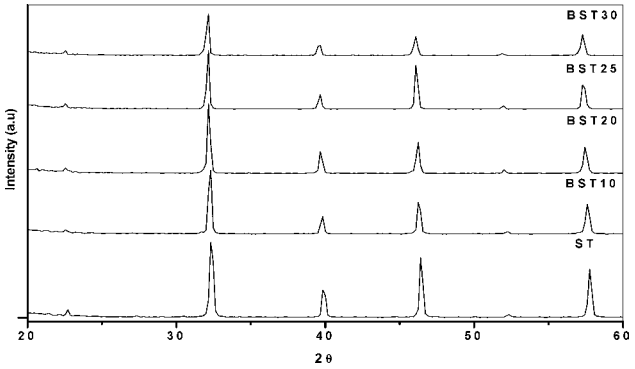

Fig. 5: XRD patterns of ST and BST with 0.2 mol% CdO as a dopant.

On the other hand, the addition of CdO to the BST20, BST25 and BST30 samples leads to a shift in the position of the XRD peaks to lower and higher diffraction angle directions, see Table 1 and fig. 6 (b-d). This means that Cd^{2+} may be located in the intermediate part of those of Ba^{2+}, $Sr^{2+}$and Ti^{4+} ions, which could be confirmed with ADSX analysis, see Table 2 and fig. 8.

Table 2: EDAX analysis of BST30 with 0.2 mol% CdO

Element	Weight%	Atomic%
O	11.05	36.88
Ti	27.19	30.32
Sr	39.70	24.20
Cd	0.17	0.08
Ba	21.90	8.52

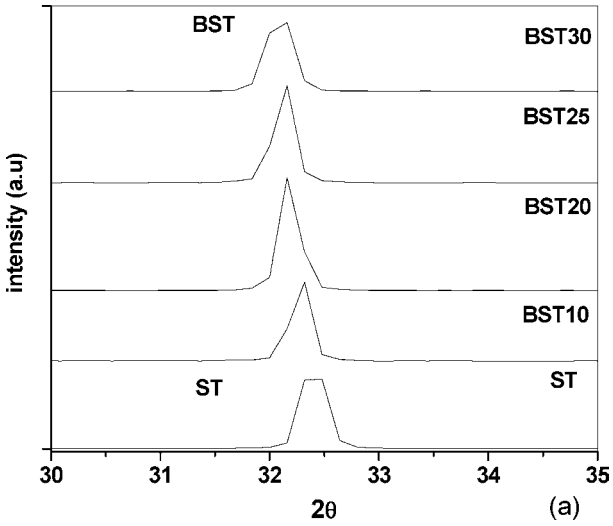

Fig. 6a: XRD patterns of sintered (Ba_xSr_{1-x}) TiO_3 ceramic bodies ($0.00 \le x \le 0.30$) with different concentration of CdO between 2θ = 30° and 2θ = 35° at pure bodies sintered at 1450 °C.

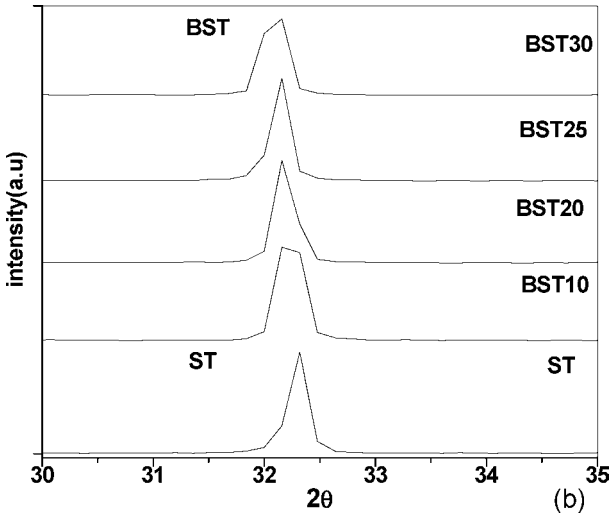

Fig. 6b: XRD patterns of sintered (Ba_xSr_{1-x}) TiO_3 ceramic bodies ($0.00 \le x \le 0.30$) with different concentration of CdO between 2θ = 30° and 2θ = 35° with 0.1 mol% CdO sintered at 1400 °C.

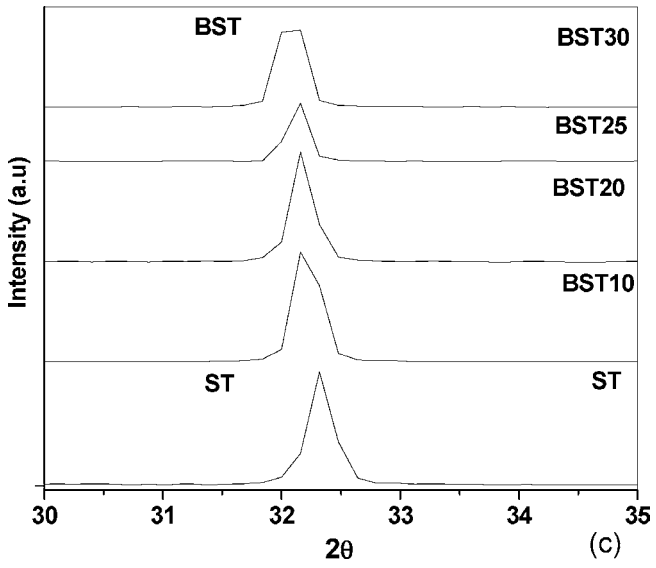

Fig. 6c: XRD patterns of sintered (Ba_xSr_{1-x}) TiO_3 ceramic bodies ($0.00 \leq x \leq 0.30$) with different concentration of CdO between 2θ = 30° and 2θ = 35° with 0.15 mol% CdO sintered at 1400 °C.

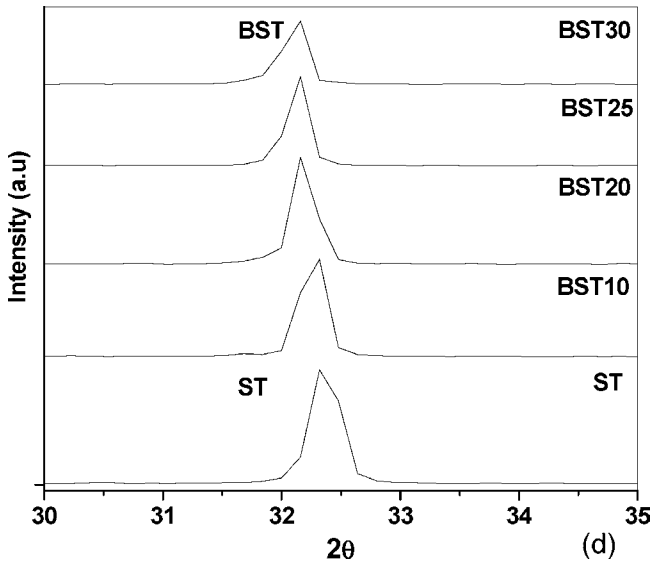

Fig. 6d: XRD patterns of sintered (Ba_xSr_{1-x}) TiO_3 ceramic bodies ($0.00 \leq x \leq 0.30$) with different concentration of CdO between 2θ = 30° and 2θ = 35° with 0.2 mol% CdO sintered at 1400 °C.

(b) ***Morphological analysis***

Fig. 7(a-t) shows the microstructure of (Ba_xSr_{1-x}) TiO_3 ceramic bodies ($0.00 \leq \times \leq 0.30$) sintered at 1450 °C and BST ceramics with different concentrations of CdO (0.00, 0.10, 0.15 and 0.20 mol %) sintered at 1400 °C. It can be seen that the grain size is non-uniform and affected by both the barium and cadmium content. Fig. 7(a) shows the micrograph of a pure ST ceramic body, which reveals that the grain size varies between 2.5 and 6 µm, and bimodal grain size distribution with monophasic morphology in support by XRD, as shown in fig. 2. However, BST ceramics with increasing Ba/Sr ratios up to $x \leq 0.25$ cause a decrease in the grain size (~4 µm), with grains that are slightly rounder in shape at x = 0.10, fig. 7(b) and at x = 0.20, see fig. 7(c) and then an increase in grain size up to (6 µm) to grains that are tetragonal in shape at x = 0.25, see fig. 7(d). Also, the microstructure of samples shows highly crystalline regular grains with a very small amount of intergranular porosity. With a further increase in Ba up to (x = 0.30) in BST30, fig. 7(e) shows a deformation in the crystalline grains, which might lead to a reduction in the microwave dielectric properties. Su et al.[13] reported that the grain size of $Ba_xSr_{1-x}TiO_3$ ceramics (x = 0.5, 0.6, 0.7 and 1 mol) increases with the Ba content or, in other words, substitution of Ba by Sr inhibits grain growth.

The effect of CdO addition on the microstructure is shown in fig. 7(f-t). The figure shows that the grains are irregularly sized, and intergranular liquid phase formation with extensive grain growth is detected for ST, BST20, BST25 and BST30 but not for BST10. This grain growth occurs with increasing CdO concentration and may be the result of the presence of oxygen vacancies in oxide systems. As is well known, the presence of oxygen vacancies in oxide systems is beneficial to mass transport during sintering. Moreover, the monotonic increase of the grain size with the CdO content, indicating that the addition of CdO mainly dissolved into the perovskite structure as confirmed by EDAX analysis of the grains of CdO added to BST30 and found to contain elements Sr, Ba, Ti, Cd and O as shown in (Table 2 and fig. 8). The CdO added to the BST10 sample, on the other hand, led to a reduction in grain size (≤ 0.1 µm), as shown in fig. 7(i-k). This can enhance its microwave dielectric properties. The reduction in grain size may be attributed to the aggressive liquid phase formed during sintering. Subsequently, the solid grains dissolve and become smaller and rounder in shape. This result is in agreement with that of Bomlai et al.[14], who showed that the decrease in the grain size of barium strontium titanate with silicon content is most probably due to the large amount of liquid phase formed during the sintering process.

(2) Physical properties

The effect of the partial substitution of Sr^{2+} by Ba^{2+} on the physical properties such as bulk density and apparent porosity at different sintering temperatures is shown in fig. 9(a-d). Ceramic bodies of ST, BST10, BST20, BST25 and BST30 sintered at 1450 °C for 2 h exhibit relatively low bulk density ranging between 4.46 and 4.73 g/cm^3 and considerably higher porosity between 4.44 and 7.35 %, fig. 9(a). On the other hand, the addition of CdO improves the densification behaviour and decreases the sintering temperature, with optimum density being obtained at 1400 °C, as shown in fig. 9(b-d). The specimens with 0.1, 0.15 and 0.2 mol % CdO show more or less the same values for bulk density (4.71 - 4.98 g/cm^3), (4.71 - 4.89 g/cm^3) and (4.63 - 4.92 g/cm^3) and apparent porosity ranging between (1.1 and 2.30 %), (0.8 and 3.30 %) and (1.2 and 3.60 %), respectively. From results obtained, it is clear that the bodies with high density values can be attributed to their lower percentage of porosity as well as uniform morphology with small grain size. However, the decrease of density values in the other samples may be attributed to the inhomogeneous grain growth with higher porosity as observed with an increase in the both Ba/Sr ratio and CdO content, see figs. 7 and 9[15, 16].

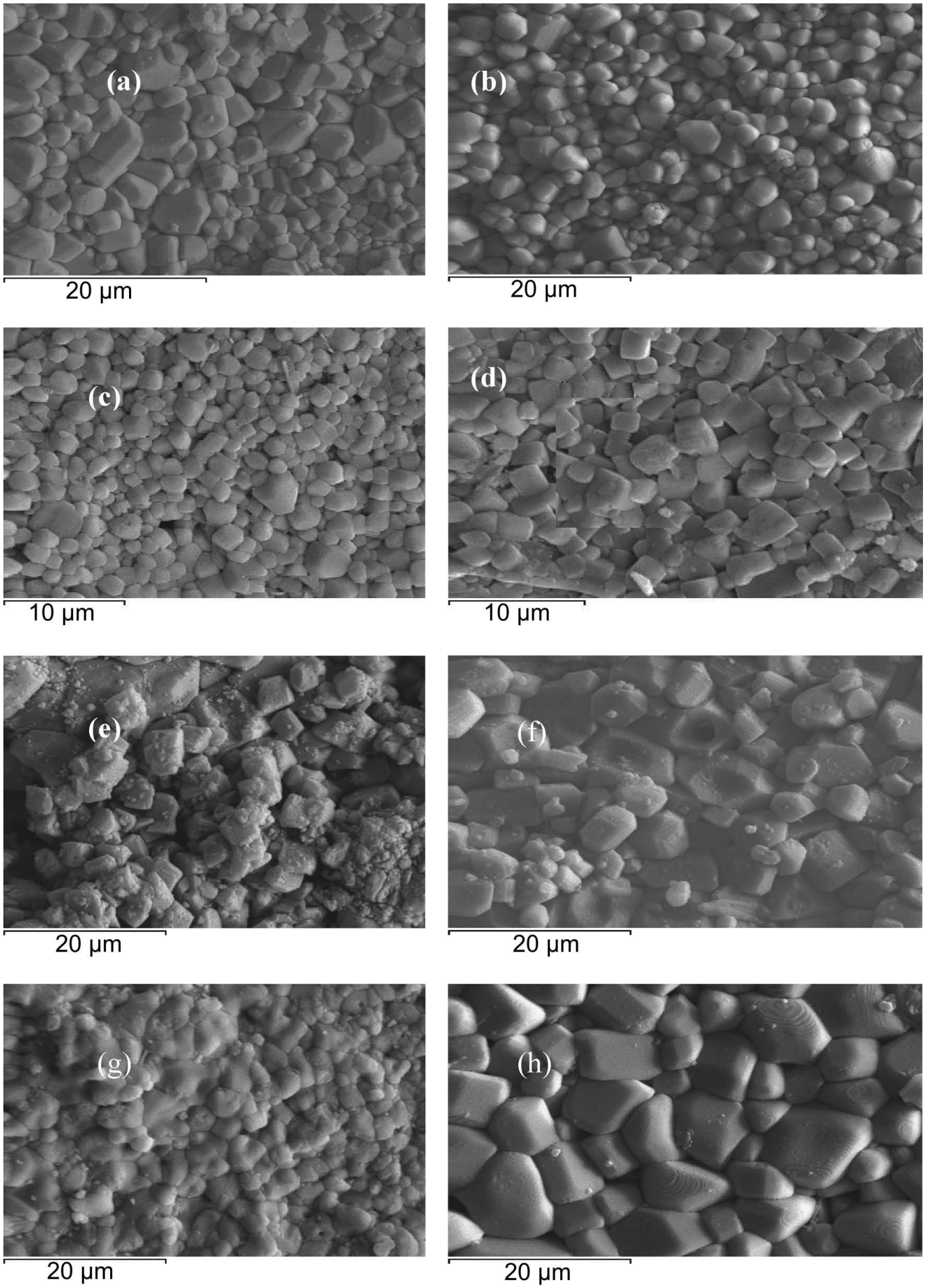
(a)
20 μm
(b)
20 μm
(c)
10 μm
(d)
10 μm
(e)
20 μm
(f)
20 μm
(g)
20 μm
(h)
20 μm

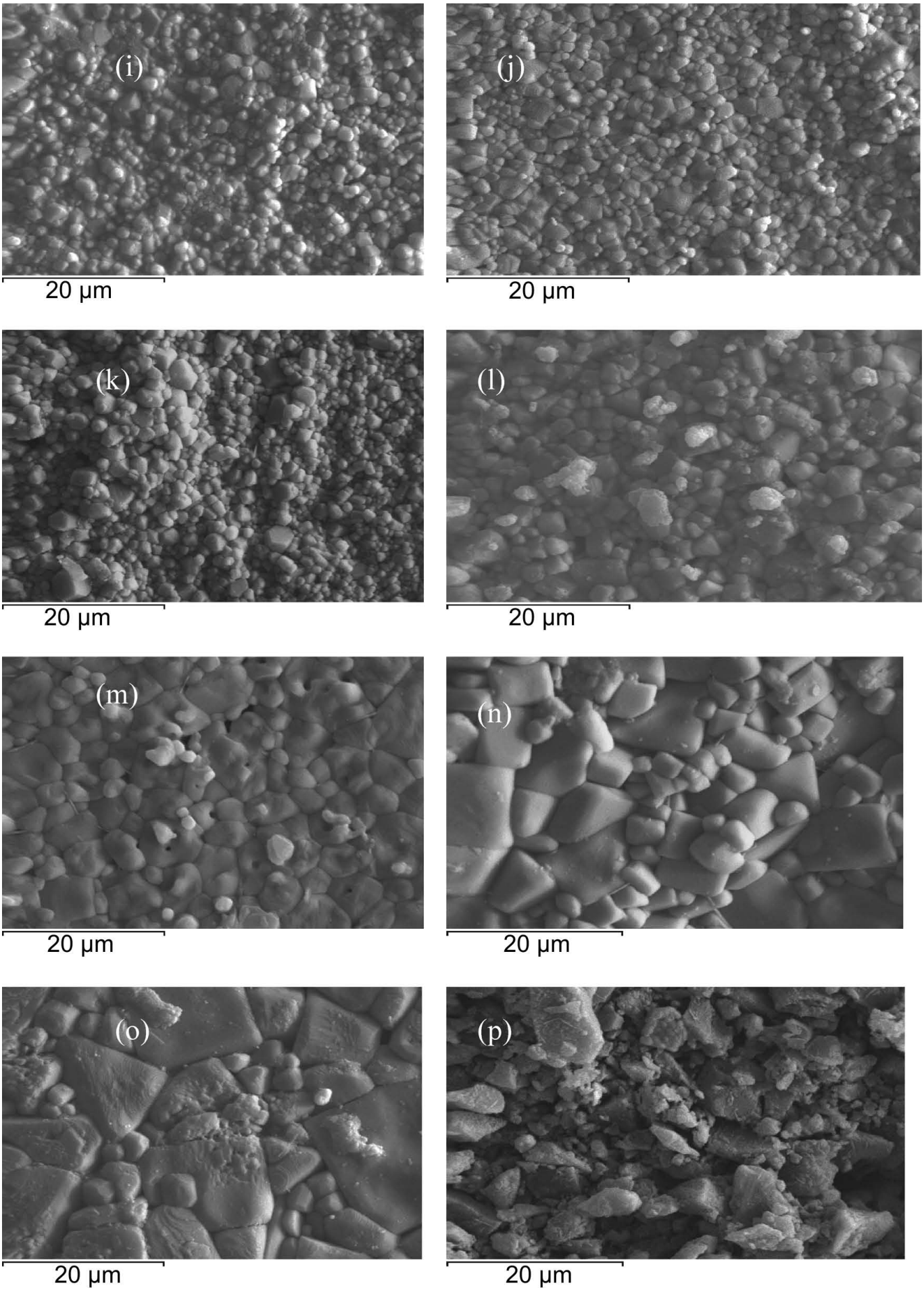
(i)
20 µm
(j)
20 µm
(k)
20 µm
(l)
20 µm
(m)
20 µm
(n)
20 µm
(o)
20 µm
(p)
20 µm

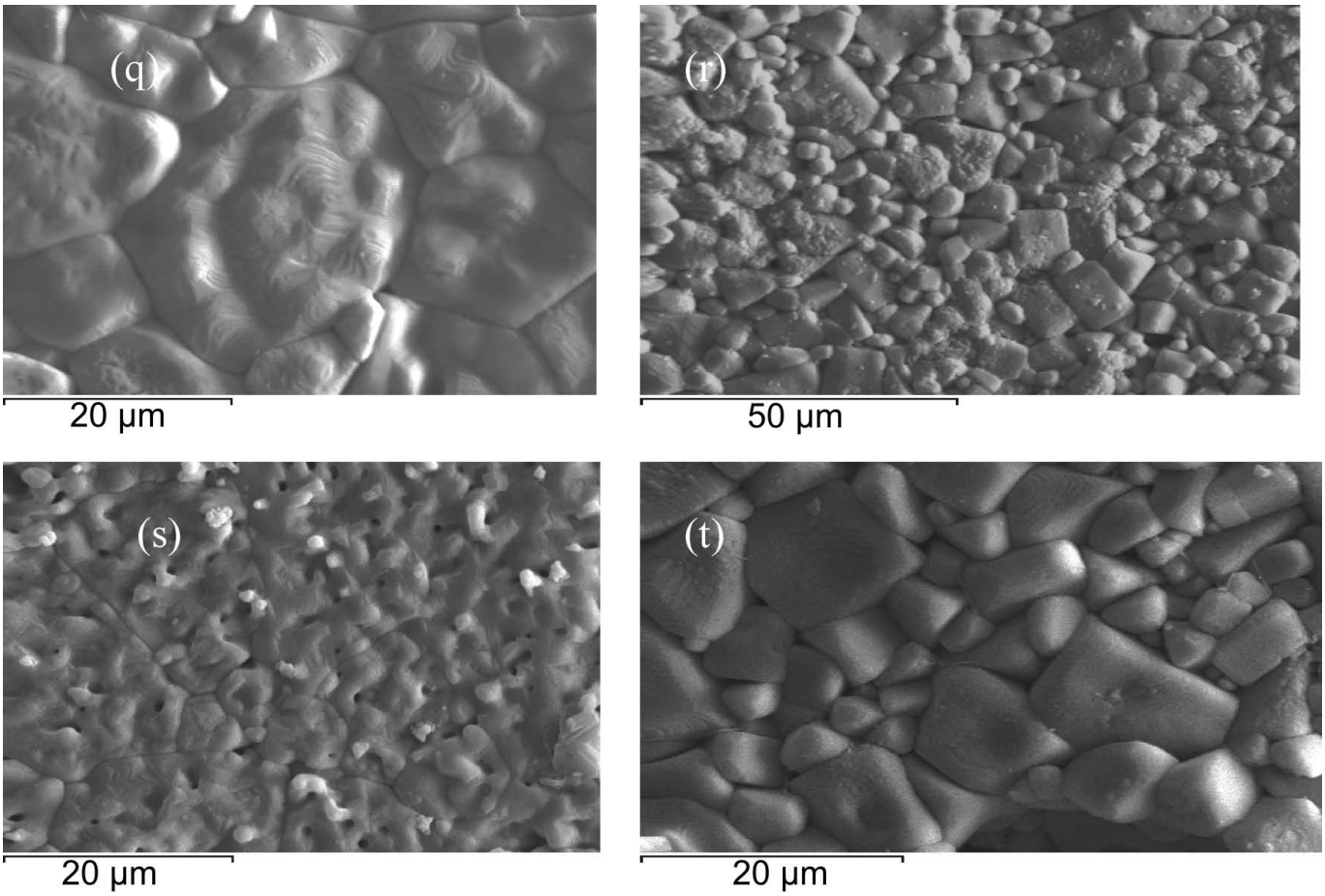

Fig. 7: Microstructure of pure (a) ST, (b) BST10, (c) BST20, (d) BST25, (e) BST30 and ceramic bodies with various CdO concentrations ST with (f) 0.1, (g) 0.15, (h) 0.2 mol% CdO , BST10 with (i) 0.1, (j) 0.15, (k) 0.2 mol% CdO, BST20 with (l) 0.1, (m) 0.15, (n) 0.2 mol% CdO, BST25 with (o) 0.1, (p) 0.15, (q) 0.2 mol% CdO and BST30 with (r) 0.1, (s) 0.15, (t) 0.2 mol% CdO.

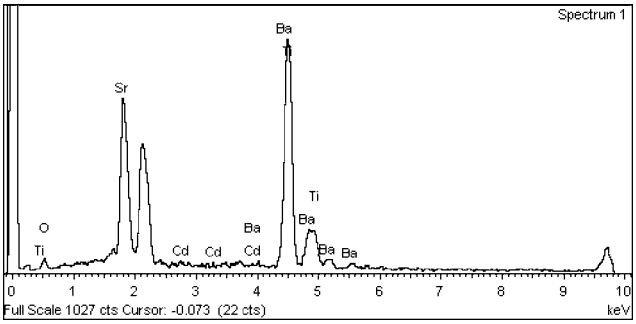

Fig. 8: Energy dispersive X-ray of BST30 with 0.2 mol% CdO.

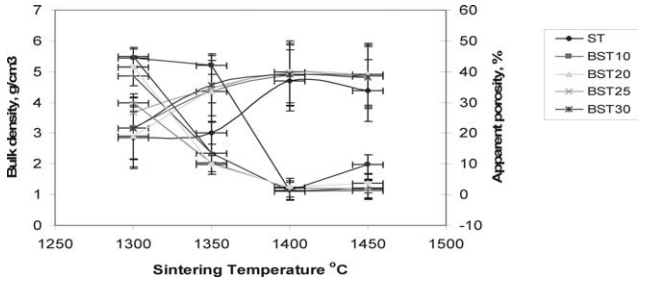

Fig. 9b: Dependence of bulk density and apparent porosity of (Ba_xSr_{1-x}) TiO_3 ceramic bodies with 0.1 mol % CdO on sintering temperature.

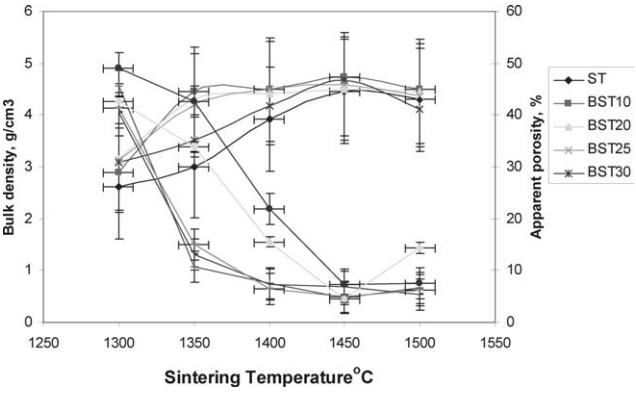

Fig. 9a: Dependence of bulk density and apparent porosity of (Ba_xSr_{1-x}) TiO_3 ceramic bodies $(0.00 \leq x \leq 0.30)$ on sintering temperature.

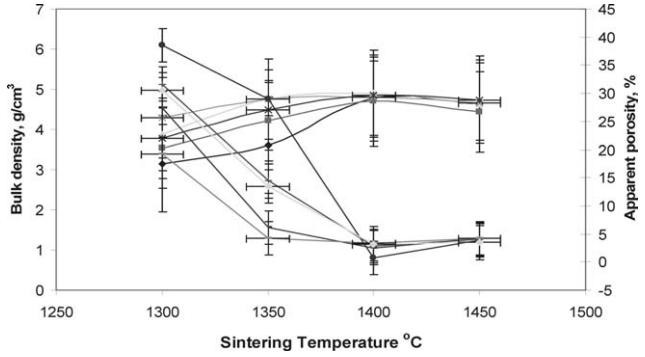

Fig. 9c: Dependence of bulk density and apparent porosity of (Ba_xSr_{1-x}) TiO_3 ceramic bodies with 0.15 mol % CdO on sintering temperature.

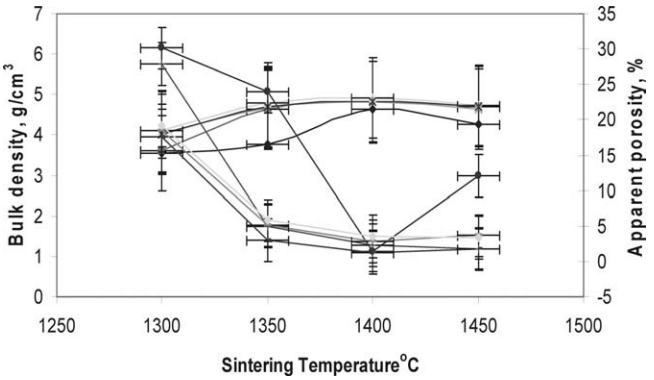

Fig. 9d: Dependence of bulk density and apparent porosity of $(Ba_xSr_{1-x})\ TiO_3$ ceramic bodies with 0.2 mol % CdO on sintering temperature.

Maximum density (4.98 g/cm^3) with a lower percentage of porosity (1 %) is therefore obtained for the BST20 ceramic body with the addition of 0.01 mol % CdO.

(3) Microwave Dielectric Properties

The dielectric properties, such as dielectric constant (ε_r), dielectric loss (DL) and quality factor ($Q \times f$), measured at microwave resonant frequency (1.4 - 2 GHZ) of both BST ceramic bodies with and without different CdO contents at optimum sintering temperature are shown in fig. 10(a-c). For pure BST ceramic bodies, the dielectric constant (ε_r) value increases from (206 to 442) with the increase in the BaO/SrO ratio. According to the Clausius-mossotti(C-M) equation, the dielectric constant increases with total dielectric polarization (αD) and decreasing unit-cell volume. Therefore, the increase of αD with Ba content owing to the ionic polarizability of Ba^{2+} ($\alpha D = 6.40$ Å^3) is higher than that of Sr^{2+} ($\alpha D = 4.24$ Å^3)[17]. So, the dielectric constant should be increased with the increase in Ba content as shown in fig. 10(a)[11].The specimens (BST) doped with CdO exhibit a high dielectric constant (ε_r), which varies from (219 to 511) at 0.10 mol %, (146 to 505) at 0.15 mol % and (183 to 491) at 0.20 mol %, depending on the CdO content, as shown in fig. 10(a). The addition of CdO significantly improves the sinterability of BST bodies. The subsequent increase in density causes an increase in the (e_r) values of the ceramic bodies[18].

The dielectric loss (DL) and quality factor ($Q \times f$) of BST specimens before and after CdO addition are shown in fig. 10(b and c). Many factors affect the microwave dielectric loss such as glassy phase, oxygen vacancies, lattice imperfection, grain size and densification or porosity. The results showed that for the pure BST specimens with an increasing Ba content from (0.00 to 0.30 mol), the quality factor ($Q \times f$) value varied from 1543 at 1.4 GHz to 2295 at 2 GHz, fig. 10(c). The increase in the dielectric loss followed by the decrease in the quality factor of BST specimens may be related to a reduction of Ti^{4+} [12, 19-21]. Liang et al.[12] concluded that the oxygen deficiency can occur in undoped BST ceramic bodies when sintered at > 1350 °C and oxygen vacancies are created according to the following equation:

$$O_o^x \rightarrow {}^1/_2O_2 + v^{\cdot\cdot}{}_o + 2e$$

The electron generated reduces Ti^{4+} to Ti^{3+} + e and produces n-type semi-conducting materials. This reduction is sufficient to cause deterioration of the dielectric loss and a reduction in the quality factor.

Moreover, the $Q \times f$ value is also significantly affected by the CdO content and the microstructure developed, as shown in figs. 7 and 10(b and c). The uniform grain morphologies yielded maximum $Q \times f$ values for each specimen prepared with a different CdO content owing to a reduction in lattice imperfection and dielectric loss[13]. Therefore, the best result is obtained for 0.2 mol % CdO in the BST10 ceramic. The growth in the developed crystalline phases may reduce the quality factor. Tsu et al.[19] found that the polarization value decreases owing to the decrease in grain size.

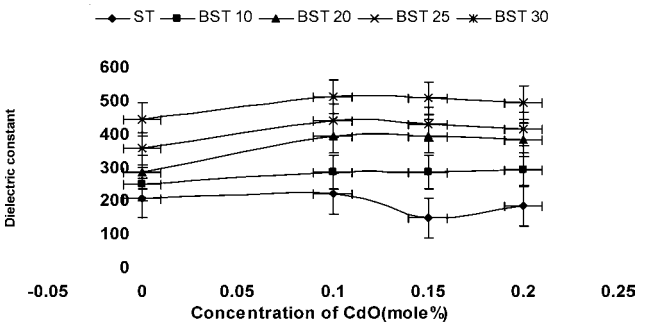

Fig. 10a: Effect of different concentration of CdO on dielectric constant of $(Ba_xSr_{1-x})\ TiO_3$ ceramic bodies.

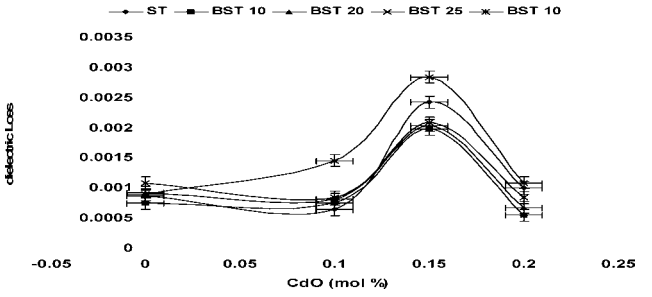

Fig. 10b: Effect of different concentration of CdO on dielectric loss of $(Ba_xSr_{1-x})\ TiO_3$ ceramic bodies.

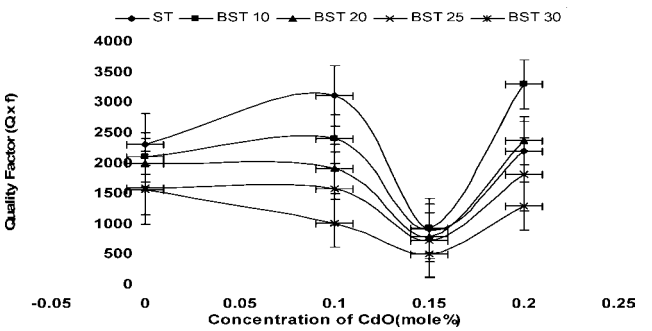

Fig. 10c: Effect of different concentration of CdO on quality factor of $(Ba_xSr_{1-x})\ TiO_3$ ceramic bodies.

The $Q \times f$ values of the other BST ceramic bodies with 0.10 and 0.20 mol % CdO are higher than those with 0.15 mol % CdO, see fig. 10(b and c). This can be attributed to the inhomogeneous grain growth with a slight increase in porosity as shown in fig. 9 (c), which leads to an increase in the dielectric loss and causes a decrease in the $Q \times f$ values[16, 22].

IV. Conclusion

From the above findings, it can be concluded that the microwave dielectric characteristics were strongly affected by the Ba/Sr ratio, cadmium content and microstructure developed. The addition of CdO (0.10, 0.15 and 0.20 mol %) to $Ba_xSr_{1-x}TiO_3$ ceramic bodies led to a reduction of sintering temperature from 1450 °C to 1400 °C and a dense microstructure. The best combination of microwave dielectric characteristics was obtained for the BST10 ceramic with 0.20 mol % CdO sintered at 1400 °C/2 h, where dielectric constant (ε_r) = 291, low dielectric loss = 0.0005 and quality factor ($Q \times f$ = 3281 at 1.8 GHz). This can be attributed to its uniform grain morphologies and fine-grained (≤ 0.1 μm) crystalline phases that are round in shape.

References

1 Wersig, W., High-frequency ceramic dielectrics and their applications for microwave components, pp.67-119 in electronic ceramic. Ed. by B. C.H. Steele. Elsevier Applied Science, London, U.K., (1991).

2 Cho, Y. S., Yoon, K. H., Dielectric ceramic, Handbook of Advanced Electronic and Photonic Materials, **4**, **5**, 175-99 Ed. By H.S. Nalwa, Academic Press, New York, (2001).

3 Kim, W. S., Kim, E. S., Yoon, K. H., Effect of Sm^{3+} substitution on dielectric properties of Ca $_{1-x}$ $Sm_{2x/3}$ TiO_3 ceramic at microwave frequencies, *J. Am. Ceram. Soc.*, **82**, 8, 2111-15, (1999).

4 Sagala, D. A., Nambu, S., Microscopic calculation of dielectric loss at microwave frequencies for complex perovskite Ba $(Zn_{1/3}Ta_{2/3})$ O_3, *J. Am. Ceram. Soc.*, **75**, 9, 2573-75, (1992).

5 Akbas, M. A., Davies, P. K., Ordering-induced microstructures and microwave dielectric properties of the Ba $(Mg_{1/3}Nb_{2/3})$ O3-$BaZrO_3$, *J. Am. Ceram. Soc.*, **81**, 3, 670-76, (1998).

6 Park, H. S., Yoon, K. H., Kim, E. S., Microwave dielectric properties and far-infrared spectrum of $(Pb_{1-x}$ $Ca_x)$ $(Fe_{0.5}$ $Ta_{0.5})$ O_3 ceramics, *J. Korean Ceram. Soc.*, **37**, 3, 256-62, (2000).

7 Flaviis, F. D., Alexopoulos, N.G., Stafsudd, O. M., Dielectric constant tunability of ZrO_2-doped barium strontium titanate for application in phased array antennas, Microwave Theory Tech., **45**, 963, 2, (1997).

8 Dimos, D., Mueller, C. H., Perovskite thin films for high-frequency capacitor applications, An. Rev. Mater. Sci. **28**, 397- 419, (1998).

9 Rhim, S. M., Hong, S, Bak, H., Kim, O. K., Effects of B_2O_3 Addition on the Dielectric and Ferroelectric Properties of $Ba_{0.7}Sr_{0.3}TiO_3$ Ceramics, *J. Am. Ceram. Soc.*, **83**, 5, 1145-48 (2000).

10 Xu, H., Karadibhave, S., Slamovich, E.B., Effects of composition on the reaction kinetics of hydrothermally derived barium strontium titanate, *J. Am. Ceram. Soc.*, **90**, 8, 2352-2357, (2007).

11 Ioachim, A., Toacsan, M. I., Banciu, M. G.,Nedelcu, L., Vasiliu, F., Alexandru, H. V., Berbecaru, C. and Stoica, G., Barium strontium titanate-based pervoskite materials for microwave applications, Progresses in Solid State Chemistry, **35**, 513-520, (2007).

12 Liang, X., Meng, Z., Wu, W., Effect of acceptor and donor dopants on the dielectric and tunable properties of barium strontium titanate, *J. Am. Ceram. Soc.*, **87**, 12, 2218-2222, (2004)

13 Su, B., Holmes, J. E., Cheng, B. L., Button, T. W., Processing effects on the microstructure and dielectric properties of barium strontium titanate (BST) ceramics. *J. Electroceram*, **9**, 111-116, (2002).

14 Bomlai, P., Sirikulrat, N., Tunkasiri, T., Microstructures and positive temperature coefficient resistivity (PTCR) characteristics of high silicon addition barium-strontium titanate ceramics. *J. Mater. Sci.*, **39**, 1831-1835, (2004).

15 Huang, C. L., Tseng, C. F., Characteristic of high Q microwave dielectric ceramics Nd $(Co_{1/2}Ti_{1/2})$ O_3 with Ca addition. *J. Am. Ceram. Soc.*, 90, **8**, 2409-2414, (2007).

16 Sun, X. F., Guo, R. S., Li, J., Preparation and properties of yttrium doped SrTiO3 anode materials Ceramic International, **34**, 219-223, (2008).

17 Moulson, A. J., Herbert, J. M., Electroceramics, materials, properties and applications, second edition John Wiley and Sons, England (2003).

18 Wu, L., Yang C., WU, J., Melting CuO in $BaTiO_3$-based System. *J. Mater. Sci. Lett.*, **11**, 1177, (1992).

19 Tsu, R., Liu, H. Y., Hsu, W.Y., Summerfelt, S., Aoki, K., Gnade, B., $Ba_{0.5}Sr_{0.5}TiO_3$ thin films deposited by PLD on SiO_2/Si RuO_2/Si and Pt/Si electrodes, Mater. Res. Soc. Symp. Proc. 361, 275, (1995).

20 Takada, T., Wang, S. F., Yoshikawa, S., Jang, J. S., Newnham, R. E., Effect on BaO-TiO_2-WO_3 microwave ceramics. *J. Am. Ceram. Soc.*, **77**, 7, 1909-1916, (1994).

21 Kim, W. D., Ko, H. K., Kwon, D. K. and Hong, K. S., Origin of microwave dielectric loss in $ZnNb_2O_6$-TiO_2, *J. Am. Ceram. Soc.*, **85**, 5, 1169-1172, (2002).

22 Lim, J. B., Jeong Y. H., Nguyen, N. H., Nahm, S., Paik, J. H., Kim J. H., Lee, and H. J., Low-temperature sintering of the $Ba_2Ti_9O_{20}$ ceramics using B_2O_3/CuO and Ba Cu(B_2O_5) additives, *J. Europ. Soc.*, **27**, 2875-2879, (2007).